Clinical Chemistry 51:2
336–345 (2005)

Proteomics and
Protein Markers

Simultaneous Measurement of β-Amyloid$_{(1–42)}$, Total Tau, and Phosphorylated Tau (Thr^{181}) in Cerebrospinal Fluid by the xMAP Technology

Annika Olsson,[1†*] Hugo Vanderstichele,[2†] Niels Andreasen,[3] Geert De Meyer,[2] Anders Wallin,[1] Björn Holmberg,[1] Lars Rosengren,[2] Eugeen Vanmechelen,[2] and Kaj Blennow[1]

Background: **To simultaneously study several biomarkers for Alzheimer disease (AD), we used the xMAP™ technology to develop and evaluate a multiparametric bead-based assay for quantification of β-amyloid$_{(1–42)}$ [Aβ$_{(1–42)}$], total tau (T-TAU), and hyperphosphorylated tau [P-TAU$_{(181P)}$] in cerebrospinal fluid (CSF).**

Methods: **We compared the new multianalyte assay format with established ELISA techniques for the same proteins. We then performed a clinical study using CSF samples from patients with AD or mild cognitive impairment with progression to AD, healthy controls, and patients with other neurologic disorders.**

Results: **The INNO-BIA AlzBio3 selectively and specifically measured Aβ$_{(1–42)}$, T-TAU, and P-TAU$_{(181P)}$ in the CSF. The new assay format had intra- and interassay CVs <10% for all analytes, even at low concentrations. The measurement range of the new assay was 3 to 4 logs compared with 1 to 2 logs for ELISAs. By plotting the mean of the values obtained in ELISA and the xMAP technology against the difference, we found that a correction factor could be used to convert xMAP results to ELISA values. The clinical study demonstrated that the new multiparametric assay could accurately distinguish patients with AD from patients with other neurologic disorders or control patients, with the diagnostic accuracy reaching recommended consensus criteria for specificity and sensitivity.**

Conclusion: **The new multiparametric method may be able to replace the corresponding ELISA methods.**

Alzheimer disease (AD),[4] the most common form of dementia, is a neurodegenerative disorder characterized by accumulation of intracellular neurofibrillary tangles and extracellular amyloid plaques throughout the cortical and limbic brain regions. The ultrastructure of neurofibrillary tangles is made up of paired helical filaments composed mainly of abnormally hyperphosphorylated tau protein (P-TAU) *(1, 2)*. The major components of the amyloid deposits are the 40- and 42-amino acid-long β-amyloid peptides [Aβ$_{(1–40)}$ and Aβ$_{(1–42)}$] *(3–5)*, which are derived from integral membrane-bound amyloid precursor protein *(6)*.

The availability of effective treatment with acetylcholine esterase inhibitors and the promise of possible future treatment with γ- and β-secretase inhibitors or vaccination regimes make early clinical diagnosis of AD important. A recent consensus report *(7)* outlined criteria for ideal biological markers for AD. Biochemical markers of AD should reflect the central pathologic features of the disease: neuronal degeneration, disturbance in β-amyloid

[1] Institute of Clinical Neuroscience, Sahlgrenska University Hospital, Mölndal, Sweden.
[2] Innogenetics N.V., Ghent, Belgium.
[3] Neurotec, Department of Geriatric Medicine, Karolinska University Hospital, Huddinge, Sweden.
*Address correspondence to this author at: Institute of Clinical Neuroscience Section, Sahlgrenska University Hospital/Mölndal, SE-431 80 Mölndal, Sweden. Fax 46-31-343-2426; e-mail Annika.Olsson@neuro.gu.se.
†These authors contributed equally to this study.
Received June 28, 2004; accepted September 28, 2004.
Previously published online at DOI: 10.1373/clinchem.2004.039347

[4] Nonstandard abbreviations: AD, Alzheimer disease; P-TAU, phosphorylated tau; Aβ, β-amyloid; CSF, cerebrospinal fluid; T-TAU, total tau; MAb, monoclonal antibody; PE, phycoerythrin; SV, streptavidin; APOE, apolipoprotein E; MCI-AD, mild cognitive impairment with progression to Alzheimer disease; FTD, frontotemporal dementia; DLB, dementia with Lewy bodies; MSA, multiple system atrophy; PD, Parkinson disease; and PSP, progressive supranuclear palsy.

metabolism with formation of plaques, and hyperphosphorylation of tau leading to formation of neurofibrillary tangles. Biological markers should have a diagnostic sensitivity ≥80% for detecting AD and a specificity ≥80% for distinguishing other dementias *(7)*. Cerebrospinal fluid (CSF) is a continuum of the interstitial fluid from the brain and spinal cord. Biochemical changes in the central nervous system are reflected in the CSF.

Several ELISAs have been developed for measurement of $A\beta_{42}$, total tau (T-TAU), and P-TAU *(8)*. In AD, the concentration of $A\beta_{42}$ in the CSF is markedly decreased *(9–14)*, whereas T-TAU *(14, 15)* and P-TAU are increased *(15–18)*. The absolute differences between the diagnostic groups are dependent on the specificity of the monoclonal antibodies (MAbs), e.g., specificity for tau phosphorylated at serine 199, threonine 181, or threonine 231, and the specificity for different $A\beta_{42}$ peptides.

The microsphere-based Luminex xMAP™ technology is a new flow cytometric method involving covalent coupling of a capture antibody to spectrally specific fluorescent microspheres *(19, 20)*. Each microsphere number is dyed with a precise concentration ratio of red- and orange-emitting fluorochromes, giving it a unique spectral identity. Classification of each bead is made by excitation at 635 nm by a first laser. Because different microsphere sets can be combined within one method and each bead number is linked with only one antibody, signals from analytes in the mixture are identified unequivocally. A third fluorochrome, phycoerythrin (PE), coupled to streptavidin (SV), quantifies the molecular reaction that has occurred at the microsphere surface. The intensity of the green fluorescence, derived after excitation of PE by a second laser at 532 nm, is reported. In comparison with conventional ELISA methods, the microsphere-based xMAP technology provides simultaneous quantification of several analytes in a small volume of sample and might also provide higher reproducibility than ELISAs *(19–21)*.

We used the Luminex xMAP technology to design a prototype multiparametric bead-based assay (INNO-BIA AlzBio3) for the simultaneous quantification in CSF of $A\beta_{(1-42)}$, T-TAU, and P-TAU phosphorylated at Thr^{181} [$P\text{-}TAU_{(181P)}$]. We first performed a comparative analysis of the new multianalyte assay format with established ELISA techniques for the same analytes *(13, 15, 22, 23)*; we then performed a clinical study using CSF samples obtained from a large sample of patients with AD or mild cognitive impairment with progression to AD (MCI-AD), healthy controls, and patients with other neurologic disorders.

Material and Methods

CHEMICALS

All reagents were of analytical grade. Synthetic peptides were obtained from Bachem, Neosytems, or AnaSpec.

ANTIBODIES AND CALIBRATORS

Antibody characterization. The characteristics of the MAbs against T-TAU (AT120 and HT7) and $P\text{-}TAU_{(181P)}$ (AT270) have been described in detail previously *(22)*. MAb 4D7A3 is a new $A\beta_{42}$-specific MAb. The diagnostic performance of an $A\beta_{(1-42)}$ assay with MAb 4D7A3 as capture antibody has been compared with an assay with the 21F12 MAb, which is used in the ELISA for $A\beta_{(1-42)}$ *(13)*. MAb 3D6 selectively binds $A\beta$ peptides with a free amino group at Asp^1 (epitope 1–5) *(13)*. The $A\beta_{(1-42)}$ specificity of the new assay has been further validated by generation of calibration curves with peptides $A\beta_{(1-42)}$, $A\beta_{(2-42)}$, and $A\beta_{(1-40)}$.

Calibrators. The calibrators for the INNO-BIA AlzBio3 assay are identical to those used in the ELISA methods for the respective markers *(13, 15, 22, 23)*, but the three calibrators are combined in one vial in the INNO-BIA AlzBio3. For each analytical run, six ready-to-use calibrators with decreasing concentrations of $A\beta_{(1-42)}$, T-TAU, and $P\text{-}TAU_{(181P)}$ were used.

We also investigated the effect of freezing and thawing on the calibrators. A multiplexed calibrator series was frozen and thawed six times. For each cycle, an aliquot of the test material was stored for at least 1 day at −20 °C. All calibrator curves were analyzed together on the immunoplate.

BEAD-BASED LUMINEX XMAP TECHNOLOGY

Although the same proteins were quantified as in the currently available ELISA methods *(13, 15, 22, 23)*, the assay format was not fully identical.

COVALENT COUPLING OF MABS

Carboxylated beads (diameter, 5.6 μm) from different microsphere numbers [region 2 for T-TAU, region 69 for $P\text{-}TAU_{(181P)}$, and region 56 for $A\beta_{(1-42)}$; lot numbers B] were chemically coupled with MAbs AT120 for T-TAU, AT270 for $P\text{-}TAU_{(181P)}$, and 4D7A3 for $A\beta_{(1-42)}$ according to the protocol from the manufacturer. The same coupling procedure was used for all MAbs. In-process control of MAb-coupling homogeneities was done by determination of (*a*) the CV for counting of 100 beads from the same region, and (*b*) the signal-to-noise ratio. Experiments included so-called nonfunctional and functional assay formats. In the nonfunctional assay, the amount of each MAb coupled to the beads was indirectly quantified by the addition of R-PE-conjugated AffinityPure $F(ab')_2$ fragment goat anti-mouse IgG (Jackson ImmunoResearch Laboratories, Lucron Products). This format gives no evidence for epitope recognition. For the functional assay, a sandwich type assay was performed.

METHODS FOR BEAD-BASED XMAP TECHNOLOGY

All incubations were performed in the dark at ambient temperature. Each well of a 96-well filter plate (Millipore Corporation) was prewetted with 250 μL of wash buffer.

The wash buffer was removed from the plates by use of a vacuum manifold (Millipore).

Before the beads were added (3000 beads per well of each protein in 100 μL of solution), they were sonicated and vortex-mixed. The buffer was then removed. A mixture of two biotinylated detector MAbs, 3D6 and HT7, was added to the wells of the filter plate (25 μL/well). The calibrators, blanks, or CSF samples were then added (75 μL/well) in duplicate and incubated overnight on a plate shaker. The plate was washed three times with 250 μL of wash buffer. SV-PE (Caltag) was added (100 μL/well) and incubated for 1 h on a plate shaker. The plate was then washed three times with 300 μL of wash buffer. Finally, 100 μL of phosphate-buffered saline was added to each well. Samples, incubated for 2 min on a plate shaker, were analyzed on the Luminex 100 IS. For each set of microspheres, 100 beads were analyzed and median values were reported.

ANALYTICAL PERFORMANCE

Curve fitting. Experiments were performed to select the best mathematical model for curve fitting, the number of dilutions included, and the concentrations of these dilutions. Evaluation was done based on model fit (R^2 values), residual analysis, and analysis of the variability on inverse prediction (i.e., estimating concentrations for unknown samples).

Method comparison and correction factors. We used CSF samples, deidentified before analysis, to calculate correction factors relating results of the xMAP method and conventional methods. For conventional results, we used ELISA measurements of $A\beta_{(1-42)}$, T-TAU, and P-$TAU_{(181P)}$ as described previously *(13, 15, 22, 23)*. We used only results that were within the analytical range of each ELISA [125–2000 ng/L for $A\beta_{(1-42)}$, 75–1200 ng/L for T-TAU, and 15.6–500 ng/L for P-$TAU_{(181P)}$]. After log transformation, the mean concentration of the two replicates was calculated for each method. The mean and the difference between the two methods were calculated for each protein for each sample *(24)*. The slope of the regression line on a difference plot (difference vs mean) revealed whether the difference between the two methods was constant (slope = 0) or changed (slope different from 0) over the assay range. In the case of a constant difference, the mean difference could be determined by use of the intercept of the horizontal regression line. We determined the correction factor for each protein by calculating the mean values for these differences and then back-transforming the results to the original scale. We also used difference plots to interpret the values after the correction factor was applied *(24)*. In addition, we calculated the interval that would contain 95% of the observed values for the assays, allowing total variabilities (CVs) of 10% for the Luminex and 10% for the ELISA.

Reproducibility. We calculated prediction error statistics for calibrators or CSF samples covering the whole concentration range of the assay. For the first part, we prepared a single-protein calibration curve. We added eight replicates of each calibrator concentration, together with the specific biotinylated antibody, to a bead mixture of four different production runs. We then calculated the intraassay CV for the calibrators as a function of the concentration *(25)*.

We determined the intraassay imprecision by duplicate analyses of at least 127 CSF samples analyzed by ELISA and xMAP. We performed a Wilcoxon matched-pairs test to calculate statistical differences for the CV values. Finally, we further evaluated reproducibility, using eight different pools of CSF samples. Different operators analyzed all these samples in different runs.

Specificity. We first verified selectivity by incubating a mixture of antibody-coupled microspheres with 0.01 μg of different biotinylated peptides, covering specific epitopes of $A\beta_{(1-42)}$, T-TAU, or P-$TAU_{(181P)}$. The sequences of the selected peptides are shown in Table 1 of the Data Supplement that accompanies the online version of this article at http://www.clinchem.org/content/vol51/issue2/ (the phosphorylated sites are indicated by bold font in the sequences). After overnight incubation at 4 °C, the antigen-antibody-bead mixture was washed three times with wash buffer, after which SV-PE was added for an additional hour. Plates were read within 30 min after termination of the reaction.

We further validated assay specificity by (*a*) performing assays with microspheres coupled to an antibody that did not recognize the proteins detected in the present assay format, (*b*) performing assays with nonspecific detector antibodies (IgG1), (*c*) performing assays with no detector antibody, (*d*) using other recombinant protein(s) in place of the calibrator, (*e*) using samples that contained only one of the calibrator proteins, and (*f*) comparing CSF values obtained with an assay with only one or a mixture of the detector antibodies (3D6 and HT7).

Determination of apolipoprotein E (APOE) alleles. We genotyped the *APOE* alleles by PCR followed by minisequencing, as described previously *(26)*.

CLINICAL STUDY

The Ethics Committees of Göteborg, Umeå, and Lund Universities approved the study. All patients or their relatives gave informed consent for participation in the study, which was performed in accordance with the provisions of the Helsinki Declaration.

Lumbar puncture was performed in the morning under standard conditions. A 12-mL CSF sample was collected and gently mixed to avoid gradient effects. All CSF samples with >500 erythrocytes/μL were excluded. All CSF samples were centrifuged to remove cells and debris,

Table 1. Clinical data and CSF analysis for the diagnostic groups.

Groups	No. of individuals (M/F)	Age,[a] years	MMSE[b] score[a]	Aß$_{(1–42)}$,[a] ng/L	T-TAU,[a] ng/L	P-TAU$_{(181P)}$,[a] ng/L
AD	78 (23/55)	78 (74–82)[c]	21 (17–25)[d]	389 (350–469)[c]	658 (492–889)[c]	106 (74–145)[c]
MCI-AD	15 (7/8)	77 (73–81)	29 (28–30)	373 (351–586)[c]	713 (466–974)[c]	88 (50–152)
Controls	53 (16/37)	72 (65–79)	29 (29–30)	698 (549–794)[e]	326 (233–422)[e]	73 (55–89)[e]
FTD	16 (5/11)	68 (62–74)[e]	22 (19–24)	720 (553–960)[e]	331 (244–477)[f]	62 (48–87)[f]
DLB	15 (9/6)	79 (76–80)	23 (19–24)	441 (393–627)	354 (205–441)[e]	56 (37–63)[e]
MSA	36 (19/17)	64 (60–71)[e]		596 (463–709)[e]	196 (138–273)[d,e]	32 (27–47)[c,e]
PD	46 (27/19)	66 (57–70)[e]		781 (569–917)[e]	179 (133–233)[c,e]	49 (38–61)[c,e]
PSP	15 (9/6)	70 (65–72)[e]		734 (650–813)[e]	219 (174–279)[e]	46 (30–57)[d,e]

[a] Median (interquartile range).
[b] MMSE, Mini Mental State Examination.
[c,d] Compared with controls: [c] $P < 0.01$; [d] $P < 0.05$.
[e,f] Compared with AD: [e] $P < 0.01$; [f] $P < 0.05$.

aliquoted, and stored at −80 °C pending biochemical analysis.

We evaluated the diagnostic performance of the new xMAP multianalyte assay with CSF samples from 78 AD patients, 15 patients with MCI-AD, 53 healthy controls, 16 patients with frontotemporal dementia (FTD), 15 patients with dementia with Lewy bodies (DLB), 36 patients with multiple system atrophy (MSA), 46 patients with Parkinson disease (PD), and 15 patients with progressive supranuclear palsy (PSP).

After calculating the sensitivity and specificity, we grouped all patients, except the AD MCI-AD patients and healthy controls, into a "neurologic disorders and other dementias" group. The clinical data for the patients are given in Table 1. In the healthy control group, symptoms or signs of psychiatric or neurologic disease were absent. The diagnosis of probable AD was made according to the National Institute of Neurological and Communicative Disorders and Stroke and Alzheimer's Disease and Related Disorders Association criteria *(27)*. No patient with AD had a family history of dementia suggestive of autosomal-dominant AD. MCI diagnoses were made according to the criteria of Petersen et al. *(28)*. The diagnosis of FTD was made according to the Lund–Manchester criteria *(29)*, diagnosis of DLB was made according to the criteria of McKeith et al. *(30)*, diagnosis of clinically definite PD was made according to the British Brain Bank diagnostic criteria *(31)*, diagnosis of clinically probable PSP was made according the criteria proposed by Golbe and Davis *(32)*, and diagnosis of clinically probable MSA was made according to the criteria proposed by Quinn *(33)*. Cognitive status was examined using the Mini Mental State Examination *(34)*.

STATISTICS

All statistical analyses in the clinical studies were performed with the Statistical Package of the Social Sciences (SPSS). Because gaussian distribution could not be obtained (Shapiro–Wilk test, $P < 0.05$) we used nonparametric statistics for the analysis. Data are given as medians (interquartile ranges). We used Kruskal–Wallis one-way ANOVA to investigate group differences followed by Dunn's test for group comparisons. Correlations were calculated with the Spearman two-tailed correlation test. Because we performed multiple correlations, we set the significance level to $P < 0.01$. We calculated the relationship between sensitivity and specificity for AD vs healthy controls by ROC curve analysis. The "optimum" cutoff value from the ROC curve is the point at which the sum of sensitivity and specificity is maximal. These calculated

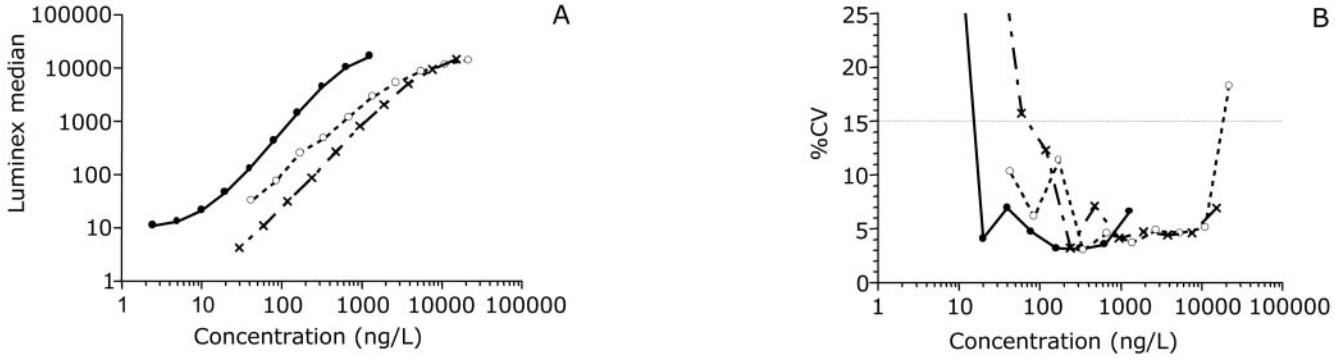

Fig. 1. Assay precision.

(*A*), calibration curves for A$\beta_{(1–42)}$ (○), T-TAU (×), and P-TAU$_{(181P)}$ (●) for the new xMAP multiparametric assay. (*B*), precision profiles showing the %CV plotted against the concentrations of the calibrators.

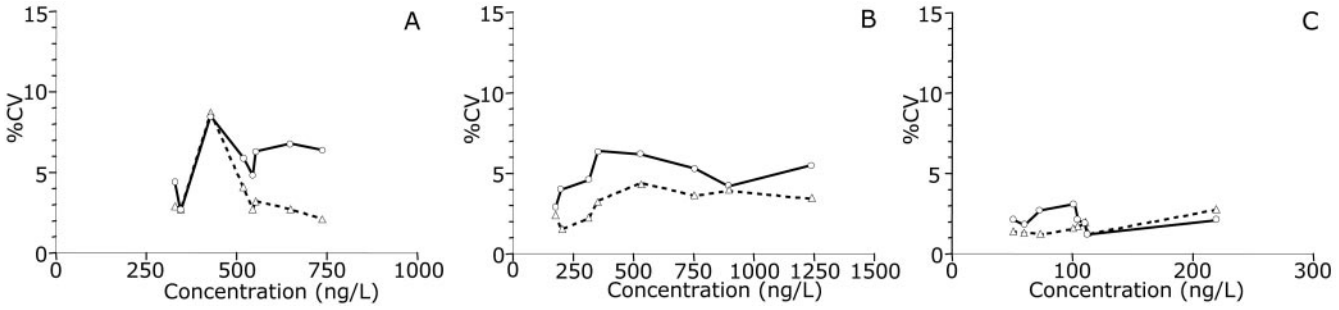

Fig. 2. Intra- (△) and interassay (○) CVs for CSF samples analyzed on the new xMAP multiparametric assay for $A\beta_{(1-42)}$ (*A*), T-TAU (*B*), and $P\text{-}TAU_{(181P)}$ (*C*).

cutoff values for each protein were also used to distinguish AD from the neurologic disorders and other dementia group and to distinguish MCI-AD patients from the control group.

Results

ANALYTICAL ASSAY PERFORMANCE

Assay calibration. Freezing and thawing of a multiplexed series of calibrators six times did not affect measured concentrations in the samples (data not shown).

Selection of the most appropriate mathematical model for curve fitting was based on experiments with calibrators with ≥10 concentrations over a wide range. Curve shapes were slightly different for the three proteins (Fig. 1A). In general, a linear model of log(Luminex median) on log concentration provided reasonable R^2 values (~0.95), but residual analysis revealed systematic biases in some parts of the assay range. Sigmoidal (four-parameter logistic) curves provided excellent fits (R^2 ≥0.99) and residuals. As a consequence, this model was selected for measurements of the three proteins. Several calibration set-ups were evaluated based on the error of inverse prediction (data not shown). A set-up with six dilutions was selected, for which the precision is described below. We observed no differences in curve fit characteristics or in hill slope values when dilution series were generated with single calibrators or with a mixture of calibrators (data not shown).

Assay precision. The precision profiles for the calibrators are shown in Fig. 1B. In contrast to classic ELISA systems, the data revealed precise measurements for each protein over the entire concentration range of the assay. The full measurement range of the assay extended over 3 to 4 logs compared with 1 to 2 logs for the ELISAs. The median (interquartile range) intraassay variability [CV, or (range × 100)/mean] was lower for the INNO-BIA AlzBio3 compared with the corresponding ELISAs: 2.0% (1.0–3.5%; n = 141) compared with 3.0% (1.0–5.0%; n = 141) for $A\beta_{(1-42)}$ (Wilcoxon matched-pairs test, P = 0.0010), 3.2% (1.2–5.6%) compared with 4.6% (2.0–7.6%; n = 127) for T-TAU (P = 0.0030), and 1.8% (0.8–3.3%) compared with 2.0% (0.7–4.3%; n = 141) for $P\text{-}TAU_{(181P)}$ (P = 0.0208).

The intra- and interassay variations for $A\beta_{(1-42)}$, T-TAU, and $P\text{-}TAU_{(181P)}$, obtained by analyzing CSF samples containing various concentrations of the proteins, are shown in Fig. 2. The low CVs indicate that precise measurements can be obtained over the entire measurement range of the assay. Even at low concentrations, CVs were <10% for all analytes. In the clinical study (n = 209), the median (10th–90th percentile) intraassay CVs were 3.8 (0.6–9.6)%, 3.6 (0.5–10)%, and 2.7 (0.6–6.8)% for $A\beta_{(1-42)}$, T-TAU, and $P\text{-}TAU_{(181P)}$, respectively.

Assay specificity. Epitope mapping results for the MAbs, obtained by use of biotinylated peptides, are shown in

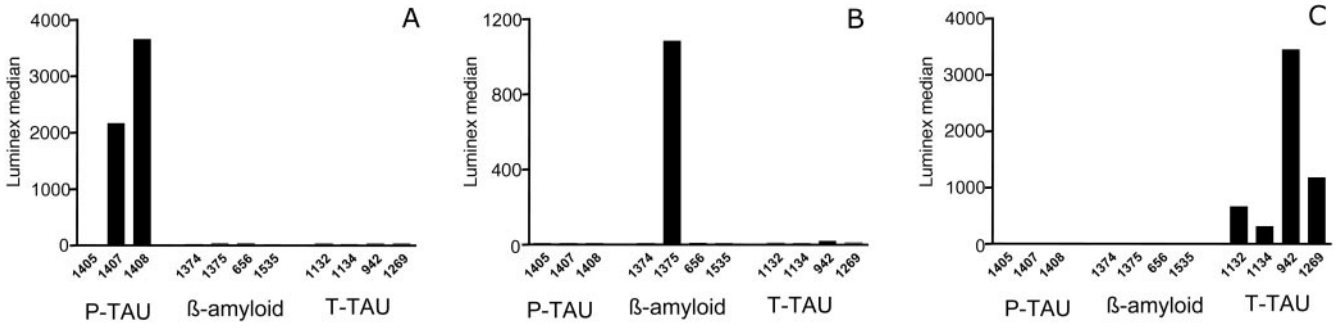

Fig. 3. Epitope mapping for mAbs AT270 (*A*), 4D7A3 (*B*), and AT120 (*C*) obtained with the biotinylated peptides listed in Table 1 of the online Data Supplement.

The peptide designations are listed on the *x axis*.

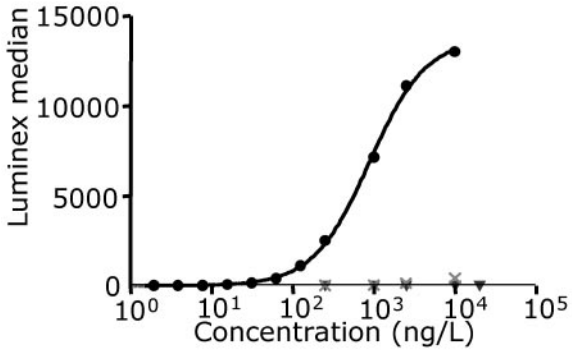

Fig. 4. Specificity of mAb 4D7A3 for peptides $A\beta_{(1-42)}$ (●), $A\beta_{(1-40)}$ (▼), and $A\beta_{(2-42)}$ (×) in a sandwich assay format with 3D6 as detector antibody.

Fig. 3. There was no obvious cross-reactivity between antibodies and peptides not containing the epitope of the protein of interest. The specificity of the AT270 MAb for P-$TAU_{(181P)}$ was confirmed by epitope mapping using synthetic peptides phosphorylated at Thr^{181} or at Thr^{175} and Thr^{181}. Moreover, when we compared results obtained by single-bead/single-antigen/single-detector antibody methods with results obtained by the complete multianalyte method, we found no significant differences between samples.

The calibration curves for peptides $A\beta_{(1-42)}$, $A\beta_{(2-42)}$, and $A\beta_{(1-40)}$ in the new xMAP multianalyte method are shown in Fig. 4. The INNO-BIA AlzBio3 is highly specific for Aβ peptides, starting at position 1 (D) and ending at position 42 (A), indicating that the new assay almost exclusively detects $A\beta_{(1-42)}$. No cross-reactivity with $A\beta_{(1-40)}$ was noted.

The assay specificity of the output signals for CSF samples for each protein was confirmed. We observed no false positivity in three CSF samples, as verified by an assay in which we replaced a microsphere coated with an antibody against one specific protein with a bead coupled to an antibody that did not recognize the protein of interest. In addition, we obtained background values when we replaced the specific biotinylated detector antibody with an antibody that did not recognize $A\beta_{(1-42)}$, tau, or P-$TAU_{(181P)}$.

Another approach to verify the assay specificity was to analyze samples with different concentrations of only one protein [$A\beta_{(1-42)}$, tau, or P-$TAU_{(181P)}$]. Results for each protein are shown in Fig. 5. Immunoreactivity was detected only on beads coupled with the specific antibodies. In other words, this approach did not reveal any cross-reactivity among proteins, confirming the assay specificity of the INNO-BIA AlzBio3. In addition, when we analyzed several CSF samples in the INNO-BIA AlzBio3, using either a mixture or only one of the two detector antibodies, we found no significant differences in concentrations, indicating an absence of cross-reactivity.

Method comparison. Shown in Fig. 6 are difference plots of log-transformed values for $A\beta_{(1-42)}$, T-TAU, and P-$TAU_{(181P)}$, which are based on analysis of at least 78 CSF samples for each protein. In each plot, the *x* axis represents the log-transformed values for the averages of concentrations obtained by both technologies, whereas the differences between methods are shown on the *y* axis. The difference plots obtained after the correction factors were applied are shown in Fig. 7. The lines represent the 95% confidence intervals, based on the assumption of a 10% CV for both the ELISA and the INNO-BIA AlzBio3. These data suggest that a constant correction factor can be used to convert results obtained with the INNO-BIA AlzBio3 to ELISA values, whereas for P-$TAU_{(181P)}$ results, a constant factor can be used only within a restricted concentration range.

CLINICAL ASSAY PERFORMANCE

A series of CSF samples from controls (n = 29) and AD patients (n = 64) were analyzed for $A\beta_{(1-42)}$ immunoreactivity, using microspheres coupled with either MAb 21F12 or MAb 4D7A3. In both cases, MAb 3D6 was used as the detector antibody. ROC analysis revealed no differences for differentiation of both diagnostic groups by these two $A\beta_{42}$-specific MAbs. The areas under the curves

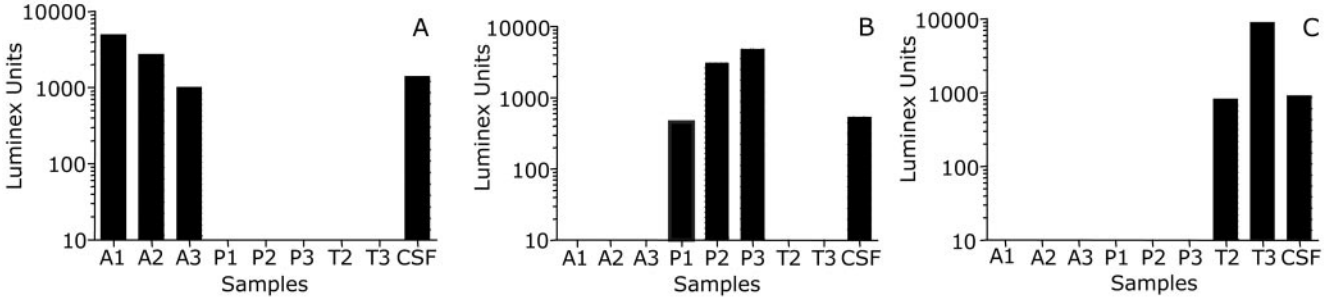

Fig. 5. Results for samples containing different concentrations of only $A\beta_{(1-42)}$ (*A1*, *A2*, and *A3*), P-$TAU_{(181P)}$ (*P1*, *P2*, and *P3*), or tau (*T2* and *T3*), together with one CSF sample, analyzed in the assay for $A\beta_{(1-42)}$ (*A*), P-$TAU_{(181P)}$ (*B*), and T-TAU (*C*).

One representative experiment is shown. Each result is the mean of two replicates. Results are expressed as Luminex units, measured on microspheres coupled with 4D7A3 antibody [$A\beta_{(1-42)}$], AT270 [P-$TAU_{(181P)}$], or AT120 (T-TAU). For more details, see the *Materials and Methods*.

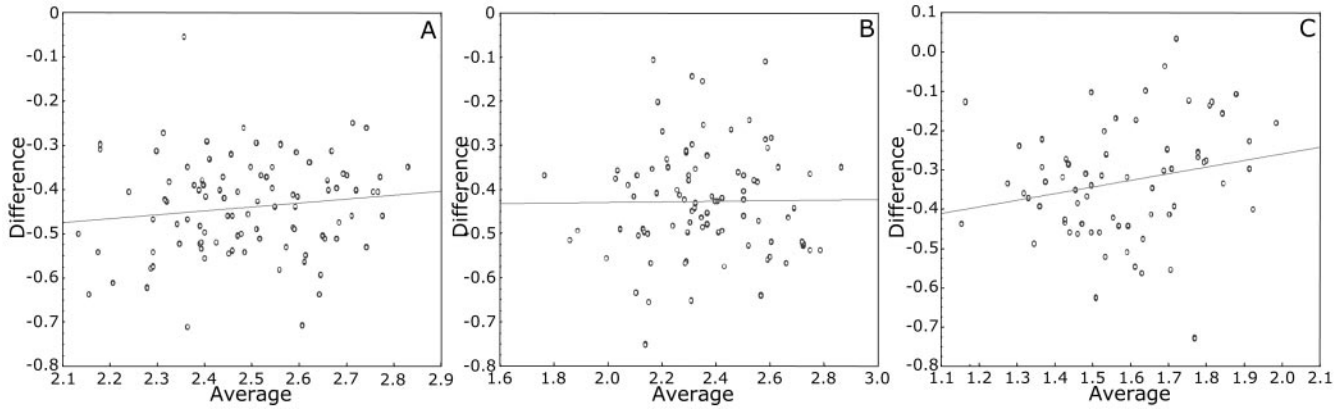

Fig. 6. Mean measured concentrations of $A\beta_{(1-42)}$ (*A*), T-TAU (*B*), and $P\text{-}TAU_{(181P)}$ (*C*) obtained with both technologies (ELISA and xMAP) (*x axis*) vs differences between the methods (*y axis*).

Shown are log-transformed values.

were 0.92 (SE = 0.036) for 21F12 and 0.914 (SE = 0.037) for 4D7A3 ($P = 0.858$).

There was a significant decrease in CSF $A\beta_{(1-42)}$ in AD patients compared with healthy controls and patients with FTD, MSA, PD, or PSP (Table 1). The concentrations of $A\beta_{(1-42)}$ in CSF were also significantly lower in patients with MCI-AD compared with controls. Both T-TAU and P-TAU were significantly increased in CSF samples from AD patients compared with healthy controls and patients with FTD, DLB, MSA, PD, and PSP. T-TAU concentrations were also significantly increased in the CSF samples from patients with MCI-AD compared with healthy controls. Finally, as shown in Table 1, the CSF-$P\text{-}TAU_{(181P)}$ concentration did not differ significantly between the MCI-AD group and the healthy control group.

Gender did not influence the CSF concentrations of any of the proteins studied in any diagnostic group (data not shown). Within the AD group, there were no significant correlations between age and CSF concentrations of $A\beta_{(1-42)}$, T-TAU, or $P\text{-}TAU_{(181P)}$. Within the AD group, there were no significant correlations between Mini Mental State Examination score and CSF concentrations of $A\beta_{(1-42)}$, T-TAU, or P-TAU.

The sensitivity and specificity for $A\beta_{(1-42)}$, T-TAU, and $P\text{-}TAU_{(181P)}$ in CSF for differentiation of AD from controls were determined by ROC curve analysis (Fig. 8). The optimum cutoffs for the three analytes were 515 ng/L for $A\beta_{(1-42)}$, 436 ng/L for T-TAU, and 87.3 ng/L for $P\text{-}TAU_{(181P)}$. The sensitivity and specificity for each protein are listed in Table 2. The individual values for each patient participating in the study are shown in Fig. 9.

In the AD group, there was a significant difference in CSF concentrations of $A\beta_{(1-42)}$ when *APOE* ϵ4 allele-positive individuals were compared with *APOE* ϵ4 allele-negative individuals ($P < 0.05$; data not shown). In contrast, there were no significant differences in either T-TAU or $P\text{-}TAU_{(181P)}$ concentrations in CSF when *APOE* ϵ4 allele-positive individuals were compared with *APOE* ϵ4 allele-negative individuals (data not shown).

Discussion

In the present study, the multiplexed bead-based xMAP technology was used for the first time for simultaneous measurement of the biomarkers $A\beta_{(1-42)}$, T-TAU, and $P\text{-}TAU_{(181P)}$ in human CSF. We showed that the new method provides diagnostic sensitivities and specificities for distinguishing AD from other neurologic disorders that are comparable to those for the already available ELISA methods [for a review, see Ref. *(8)*].

The xMAP technology provides several potential ana-

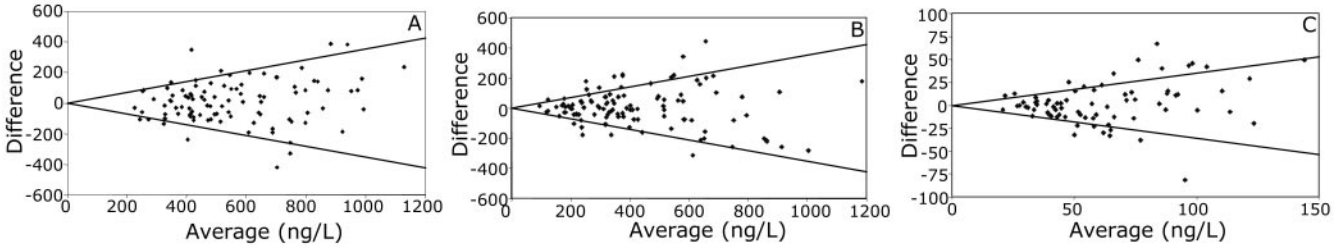

Fig. 7. Mean measured concentrations of $A\beta_{(1-42)}$ (*A*), T-TAU (*B*), and $P\text{-}TAU_{(181P)}$ (*C*) obtained with both technologies (ELISA and xMAP) (*x axis*) vs differences between the methods (*y axis*).

Values after application of the correction factor for each protein.

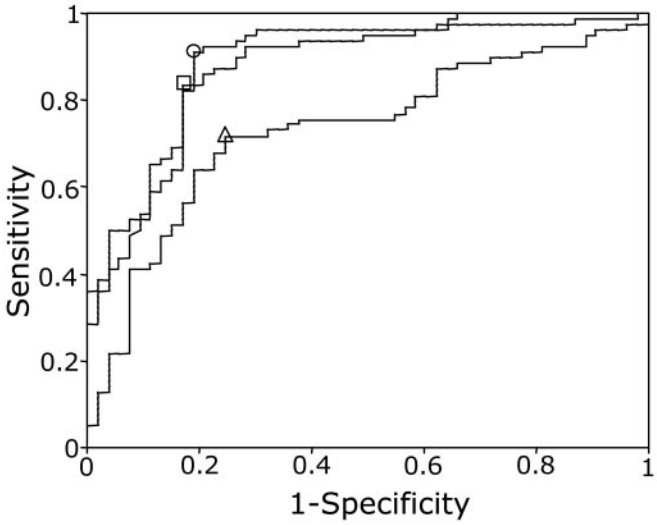

Fig. 8. ROC curve analysis for $A\beta_{(1-42)}$, T-TAU, and P-$TAU_{(181P)}$ in CSF for differentiation of AD patients from healthy controls.

The optimum cutoffs were 515 ng/L for $A\beta_{(1-42)}$ (○), 436 ng/L for T-TAU (□), and 87.3 ng/L for P-$TAU_{(181P)}$ (△).

lytical and clinical advantages over the conventional ELISA methods. The reductions in total assay time as well as in the number of handling steps make this a cost-effective assay system for clinical laboratories. Only small volumes of biological samples are required for simultaneous quantification of all analytes. The heterogeneous etiology of AD and other neurodegenerative disorders will most probably require combined measurement of several biomarkers, each reflecting a specific pathogenic mechanism for the different disorders. The discriminative power could be further improved by adding other CSF biomarkers, including but not limited to S100β, N-terminally truncated variants of Aβ peptides, and α-synuclein, into a CSF panel. The xMAP technology provides a tool for analyzing all of these markers in a single CSF sample, which could improve clinical diagnosis of AD and other neurodegenerative disorders.

Table 2. Comparisons between AD, MCI-AD, and other groups.[a]

Marker	Controls (n = 53) vs AD (n = 78)	Neurologic disease (n = 128) vs AD (n = 78)	Controls (n = 53) vs MCI-AD (n = 15)
$A\beta_{(1-42)}$			
AUC	0.892		
SE	0.030		
Cutoff, ng/L	515	515	515
Sensitivity, %	91		67
Specificity, %	81	75	
T-TAU			
AUC	0.873		
SE	0.032		
Cutoff, ng/L	436	436	436
Sensitivity, %	83		80
Specificity, %	83	89	
P-$TAU_{(181P)}$			
AUC	0.732		
SE	0.045		
Cutoff, ng/L	87.3	87.3	87.3
Sensitivity, %	72		53
Specificity, %	76	95	

[a] ROC curve analysis with area under the curve (AUC) and SE calculated using Statistical Package of the Social Science (SPSS). Cutoff is given for sensitivity + specificity maximized for AD vs controls.

To allow implementation of the new assay format in routine clinical practice, it was essential that we compare it with currently available methodologies. By plotting the mean of the values obtained by ELISA and the xMAP technology against the difference, we found that a constant factor could be used to convert xMAP results to ELISA values for $A\beta_{(1-42)}$, T-TAU, and P-$TAU_{(181P)}$. However, for P-$TAU_{(181P)}$, the constant correction factor was limited to a smaller concentration range in the xMAP test. There are several reasons that the absolute values obtained by the two technologies are different, including the selected pairs of antibodies, the method for presenting the antibodies, different accessibilities of the epitopes of the antibodies, different incubation conditions for some of the proteins, and differences in the slopes of the calibrator curves. These differences are not linked to the multiplexing character of the assay format because there were no obvious differences when multiplexed assays were compared with single-protein testing.

Because of the multiplexed format of the new assay, verification of a lack of cross-reactivity for each protein was very important. Epitope mapping clearly showed no cross-reactivity between the MAbs coupled to microspheres and peptides that did not contain the epitope. The analytical specificity of the new assay was further confirmed by the absence of any statistical difference in results for CSF samples when assayed in the single-bead, single-antigen, single-detector antibody format compared with the new multianalyte assay.

Precision profiling experiments revealed that assay variability was lower over the entire measurement range for the xMAP assay compared with the currently used ELISA tests. This low variability reduced the need to predilute CSF samples before analysis, allowing analysis of samples from patients with a broad spectrum of clinical symptoms. This is related in part to the ready-to-use series of calibrators for each protein, which limits potential errors introduced by preparation of calibrators from highly concentrated stock solutions. In addition, the multiplexed calibrator series can be frozen several times without affecting the outcome of the test. Furthermore, the technology itself, in which the final result is the median value of the analysis of hundreds of microspheres of a specific region, gives a more robust signal.

In agreement with several previous reports, we found a decrease in CSF $A\beta_{(1-42)}$ in AD patients compared with healthy controls and patients with FTD, MSA, PD, or PSP

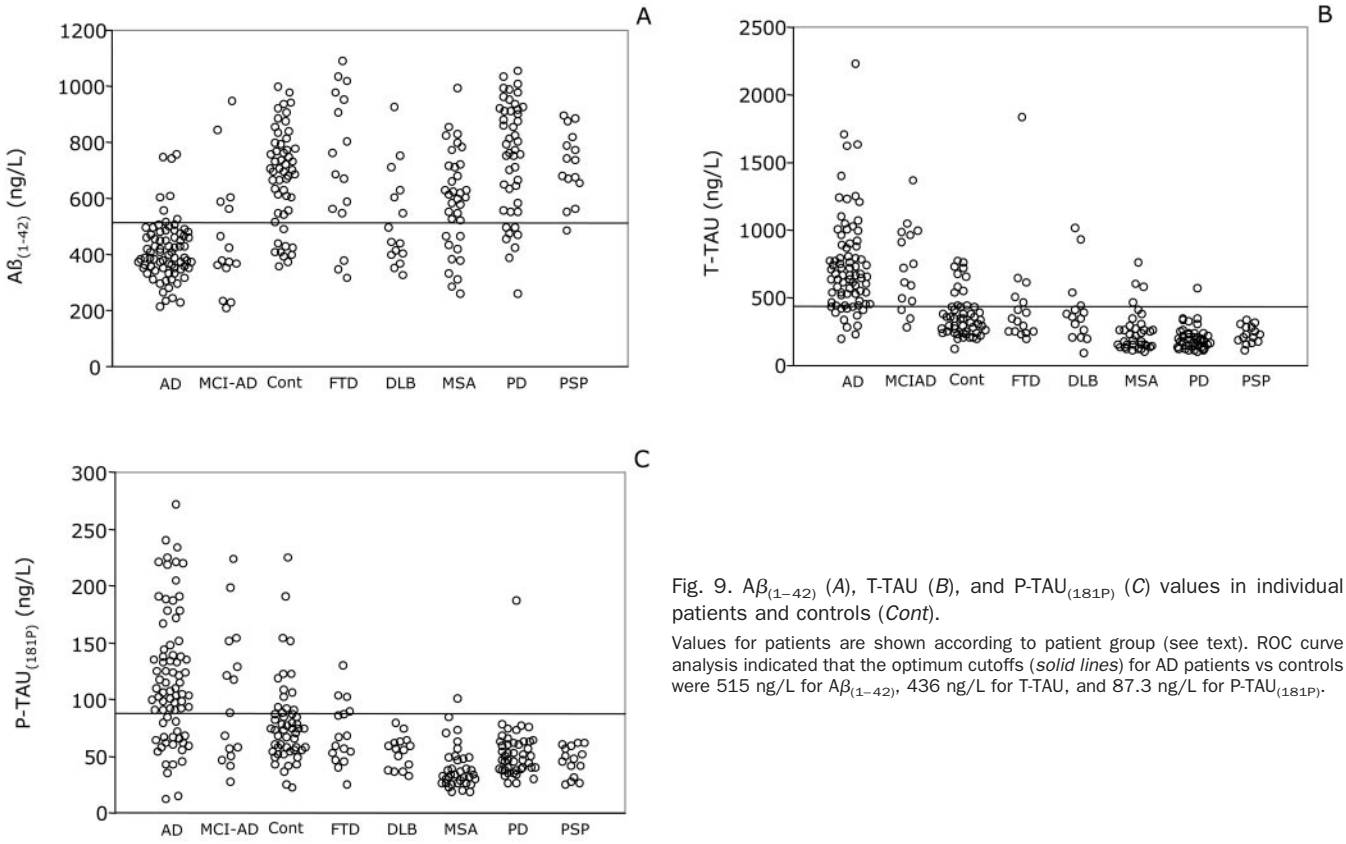

Fig. 9. A$\beta_{(1-42)}$ (*A*), T-TAU (*B*), and P-TAU$_{(181P)}$ (*C*) values in individual patients and controls (*Cont*).

Values for patients are shown according to patient group (see text). ROC curve analysis indicated that the optimum cutoffs (*solid lines*) for AD patients vs controls were 515 ng/L for A$\beta_{(1-42)}$, 436 ng/L for T-TAU, and 87.3 ng/L for P-TAU$_{(181P)}$.

(9–14). Furthermore, and in agreement with several previous reports, we found that the concentrations of T-TAU and P-TAU$_{(181P)}$ in CSF from AD patients were higher than in controls and in each group within the neurologic disorders and other dementia group *(14–18)*. The consistency of our results with results from previous clinical studies indicate that the new xMAP technology may be a suitable replacement for the ELISA methods used today for quantification of A$\beta_{(1-42)}$, T-TAU, and P-TAU$_{(181P)}$ in CSF. We also found decreased A$\beta_{(1-42)}$ and increased T-TAU in CSF samples from MCI-AD patients compared with controls. These findings are consistent with a previous study on MCI-AD patients, suggesting that concentrations of these CSF markers are abnormal before the onset of clinical dementia *(35)*.

Inheritance of the *APOE* ϵ4 allele increases the risk of sporadic AD *(36)*. We therefore analyzed possible effects of *APOE* ϵ4 on CSF concentrations of A$\beta_{(1-42)}$, T-TAU, and P-TAU$_{(181P)}$. Within the AD group, we found that neither T-TAU nor P-TAU$_{(181P)}$ varied according to *APOE* genotype. In contrast, we found that the A$\beta_{(1-42)}$ concentration in CSF varied according to *APOE* genotype; with lower CSF A$\beta_{(1-42)}$ concentrations in individuals with higher numbers of the *APOE* ϵ4 allele. This finding is in agreement with a recent study on more than 500 AD patients *(37)*.

We are grateful to Maria Lindbjer-Andersson and Vicky Mortier for excellent technical assistance. This work was supported by grants from the Swedish Research Council (Grant K2004-33X-14002-04A), Alzheimerfonden, and Stiftelsen för Gamla Tjänarinnor.

References

1. Kosik KS, Joachim CL, Selkoe DJ. Microtubule-associated protein tau (tau) is a major antigenic component of paired helical filaments in Alzheimer disease. Proc Natl Acad Sci U S A 1986;83:4044–8.
2. Grundke-Iqbal I, Iqbal K, Tung YC, Quinlan M, Wisniewski HM, Binder LI. Abnormal phosphorylation of the microtubule-associated protein tau (tau) in Alzheimer cytoskeletal pathology. Proc Natl Acad Sci U S A 1986;83:4913–7.
3. Glenner GG, Wong CW. Alzheimer's disease: initial report of the purification and characterization of a novel cerebrovascular amyloid protein. Biochem Biophys Res Commun 1984;120:885–90.
4. Tamaoka A, Kondo T, Odaka A, Sahara N, Sawamura N, Ozawa K, et al. Biochemical evidence for the long-tail form (Aβ1–42/43) of amyloid β protein as a seed molecule in cerebral deposits of Alzheimer's disease. Biochem Biophys Res Commun 1994;205:834–42.
5. Iwatsubo T, Odaka A, Suzuki N, Mizusawa H, Nukina N, Ihara Y. Visualization of Aβ42(43) and Aβ40 in senile plaques with end-specific Aβ monoclonals: evidence that an initially deposited species is Aβ42(43). Neuron 1994;13:45–53.
6. Kang J, Lemaire HG, Unterbeck A, Salbaum JM, Masters CL, Grzeschik KH, et al. The precursor of Alzheimer's disease amyloid

A4 protein resembles a cell-surface receptor. Nature 1987;325:733–6.
7. Consensus report of the Working Group on: "Molecular and Biochemical Markers of Alzheimer's Disease. The Ronald and Nancy Reagan Research Institute of the Alzheimer's Association and the National Institute on Aging Working Group [Erratum published in: Neurobiol Aging 1998;19:285]. Neurobiol Aging 1998;19:109–16.
8. Blennow K, Hampel H. CSF markers for incipient Alzheimer's disease. Lancet Neurol 2003;2:605–13.
9. Andreasen N, Hesse C, Davidsson P, Minthon L, Wallin A, Winblad B, et al. Cerebrospinal fluid β-amyloid(1–42) in Alzheimer disease. Differences between early- and late-onset Alzheimer disease and stability during the course of disease. Arch Neurol 1999;56:673–80.
10. Sjögren M, Minthon L, Davidsson P, Granérus AK, Clarberg A, Vanderstichele H, et al. CSF levels of tau, β-amyloid(1–42) and GAP-43 in frontotemporal dementia, other types of dementia and normal aging. J Neural Transm 2000;107:563–79.
11. Hulstaert F, Blennow K, Ivanoiu A, Schoonderwaldt HC, Riemenschneider M, De Deyn PP, et al. Improved discrimination of AD patients using β-amyloid(1–42) and tau levels in CSF. Neurology 1999;52:1555–62.
12. Kanai M, Matsubara E, Isoe K, Urakami K, Nakashima K, Arai H, et al. Longitudinal study of cerebrospinal fluid levels of tau, Aβ1–40, and Aβ1–42(43) in Alzheimer's disease: a study in Japan. Ann Neurol 1998;44:17–26.
13. Vanderstichele H, Van Kerschaver E, Hesse C, Davidsson P, Buyse MA, Andreasen N, et al. Standardization of measurement of β-amyloid(1–42) in cerebrospinal fluid and plasma. Amyloid 2000;7:245–58.
14. Motter R, Vigo-Pelfrey C, Kholodenko D, Barbour R, Johnson-Wood K, Galasko D, et al. Reduction of β-amyloid peptide42 in the cerebrospinal fluid of patients with Alzheimer's disease. Ann Neurol 1995;38:643–8.
15. Blennow K, Wallin A, Ågren H, Spenger C, Siegfried J, Vanmechelen E. Tau protein in cerebrospinal fluid: a biochemical marker for axonal degeneration in Alzheimer disease? Mol Chem Neuropathol 1995;26:231–45.
16. Kohnken R, Buerger K, Zinkowski R, Miller C, Kerkman D, DeBernardis J, et al. Detection of tau phosphorylated at threonine 231 in cerebrospinal fluid of Alzheimer's disease patients. Neurosci Lett 2000;287:187–90.
17. Buerger K, Zinkowski R, Teipel SJ, Tapiola T, Arai H, Blennow K, et al. Differential diagnosis of Alzheimer disease with cerebrospinal fluid levels of tau protein phosphorylated at threonine 231. Arch Neurol 2002;59:1267–72.
18. Ishiguro K, Ohno H, Arai H, Yamaguchi H, Urakami K, Park JM, et al. Phosphorylated tau in human cerebrospinal fluid is a diagnostic marker for Alzheimer's disease. Neurosci Lett 1999;270:91–4.
19. Gordon RF, McDade RL. Multiplexed quantification of human IgG, IgA, and IgM with the FlowMetrix system. Clin Chem 1997;43:1799–801.
20. Oliver KG, Kettman JR, Fulton RJ. Multiplexed analysis of human cytokines by use of the FlowMetrix system. Clin Chem 1998;44:2057–60.
21. Prabhakar U, Eirikis E, Davis HM. Simultaneous quantification of proinflammatory cytokines in human plasma using the LabMAP assay. J Immunol Methods 2002;260:207–18.
22. Vanmechelen E, Vanderstichele H, Davidsson P, Van Kerschaver E, Van Der Perre B, Sjögren M, et al. Quantification of tau phosphorylated at threonine 181 in human cerebrospinal fluid: a sandwich ELISA with a synthetic phosphopeptide for standardization. Neurosci Lett 2000;285:49–52.
23. Vandermeeren M, Mercken M, Vanmechelen E, Six J, van de Voorde A, Martin JJ, et al. Detection of tau proteins in normal and Alzheimer's disease cerebrospinal fluid with a sensitive sandwich enzyme-linked immunosorbent assay. J Neurochem 1993;61:1828–34.
24. Petersen PH, Stöckl D, Blaabjerg O, Pedersen B, Birkemose E, Thienpont L, et al. Graphical interpretation of analytical data from comparison of a field method with reference method by use of difference plots. Clin Chem 1997;43:2039–46.
25. Dudley RA, Edwards P, Ekins RP, Finney DJ, McKenzie IG, Raab GM, et al. Guidelines for immunoassay data processing. Clin Chem 1985;31:1264–71.
26. Blennow K, Ricksten A, Prince JA, Brookes AJ, Emahazion T, Wasslavik C, et al. No association between the α2-macroglobulin (A2M) deletion and Alzheimer's disease, and no change in A2M mRNA, protein, or protein expression. J Neural Transm 2000;107:1065–79.
27. McKhann G, Drachman D, Folstein M, Katzman R, Price D, Stadlan EM. Clinical diagnosis of Alzheimer's disease: report of the NINCDS-ADRDA Work Group under the auspices of Department of Health and Human Services Task Force on Alzheimer's Disease. Neurology 1984;34:939–44.
28. Petersen RC, Smith GE, Waring SC, Ivnik RJ, Tangalos EG, Kokmen E. Mild cognitive impairment: clinical characterization and outcome. Arch Neurol 1999;56:303–8.
29. Clinical and neuropathological criteria for frontotemporal dementia. The Lund and Manchester Groups. J Neurol Neurosurg Psychiatry 1994;57:416–8.
30. McKeith IG, Galasko D, Kosaka K, Perry EK, Dickson DW, Hansen LA, et al. Consensus guidelines for the clinical and pathologic diagnosis of dementia with Lewy bodies (DLB): report of the consortium on DLB international workshop. Neurology 1996;47:1113–24.
31. Hughes AJ, Daniel SE, Kilford L, Lees AJ. Accuracy of clinical diagnosis of idiopathic Parkinson's disease: a clinico-pathological study of 100 cases. J Neurol Neurosurg Psychiatry 1992;55:181–4.
32. Golbe L, Davis P. Progressive supranuclear palsy. In: Jankovic J, Tolosa E, eds. Parkinson's disease and movement disorders. Baltimore: Williams and Wilkins, 1993:145–61.
33. Quinn N. Multiple system atrophy-the nature of the beast. J Neurol Neurosurg Psychiatry 1989;Suppl:78–89.
34. Folstein MF, Folstein SE, McHugh PR. "Mini-mental state". A practical method for grading the cognitive state of patients for the clinician. J Psychiatr Res 1975;12:189–98.
35. Andreasen N, Minthon L, Vanmechelen E, Vanderstichele H, Davidsson P, Winblad B, et al. Cerebrospinal fluid tau and Aβ42 as predictors of development of Alzheimer's disease in patients with mild cognitive impairment. Neurosci Lett 1999;273:5–8.
36. Saunders AM, Strittmatter WJ, Schmechel D, George-Hyslop PH, Pericak-Vance MA, Joo SH, et al. Association of apolipoprotein E allele epsilon 4 with late-onset familial and sporadic Alzheimer's disease. Neurology 1993;43:1467–72.
37. Prince JA, Zetterberg H, Andreasen N, Marcusson J, Blennow K. The APOE ϵ4 allele is associated with reduced cerebrospinal fluid levels of Aβ42. Neurology 2004;62:2116–8.